

1
2
3
4
5
6
7
8
9
10
11
12
13
14
15
16

Reversing Sahelian Droughts

Authors: Katharine Ricke^{1,2}, Detelina Ivanova¹, Taylor McKie¹, Maria Rugenstein³

¹ Scripps Institution of Oceanography, La Jolla CA 92037

² School of Global Policy & Strategy, UC San Diego, La Jolla CA 92037

³ Department of Atmospheric Science, Colorado State University

Corresponding author: Katharine Ricke (kricke@ucsd.edu)

Key Points:

- Earth system model simulations indicate cooling the Indian Ocean with artificial upwelling would increase precipitation in the Sahel
- Our intervention can reverse the mid-20th century Sahelian drought, but has side effects in other regions such as sub-Saharan East Africa
- The energy and infrastructure for large-scale regional artificial upwelling would likely be costly and require a major actor to implement

17 **Abstract**

18 Earth system modeling of climate geoengineering proposals suggests that the physical outcomes
19 of such interventions will depend on the particulars of the implementation. Here, we present a
20 first attempt to “geoengineer” a well-known teleconnection between sea surface temperatures
21 (SSTs) and Sahelian precipitation. Using idealized earth system model simulations, we show that
22 selectively cooling the Indian Ocean efficiently increases precipitation in the Sahel region,
23 widening the seasonally migrating rainband over Africa. Applying the SST perturbations derived
24 from the idealized experiments to observationally constrained historical ones, we find that our
25 intervention can reverse conditions as extreme as the mid-20th century Sahelian drought, albeit
26 less efficiently than in the idealized simulations. Side effects include changes in the seasonal
27 distribution of Sahelian precipitation and substantial precipitation reductions in sub-Saharan East
28 Africa. This work represents a proof-of-concept illustration of effects that might be expected
29 with a tailored, regional approach to climate intervention.

30 **Plain Language Summary**

31 Climate geoengineering is the idea that some impacts of anthropogenic climate change could be
32 reduced through deliberate, engineered intervention into the Earth system. Research on this topic
33 has generally focused on global approaches that would have diffuse effects on the climate, but
34 regional approaches may be more geopolitically feasible and have been little researched. We
35 investigate whether a regional climate intervention, in this case cooling the Indian Ocean with
36 pipes that bring deep cool water to the surface, could be designed to reverse a particular climate
37 impact. We show that Indian Ocean cooling can increase precipitation in the Sahel region of
38 Africa. We illustrate the implications of this by using computer simulations of our designed
39 intervention to reverse a drought in the Sahel that happened in the 20th century. While we are
40 able to reverse the drought, increasing precipitation in the Sahel also decreases precipitation in
41 sub-Saharan East Africa. A feasibility assessment indicates that millions of pipes would likely be
42 required to implement wide-scale cooling of the Indian Ocean.

43 **1 Designing a regional climate intervention**

44 The past ten years has seen an increasing body of research devoted to climate geoengineering
45 technologies – approaches that would deliberately modify the earth’s climate system to reduce

46 some effects or impacts associated with global warming ([Boettcher et al., 2019](#)). While most of
47 the proposals have aimed to make global-scale forcing interventions, a recent government-
48 funded cloud brightening experiment off the eastern coast of Australia ([Readfearn, 2020](#)) as well
49 as a large-scale proposed weather modification program in China ([Griffiths, 2020](#)), suggest that
50 some decision makers are closely considering unconventional options for mitigating the risks
51 presented by climate change. Climate geoengineering presents an imperfect opportunity to
52 circumvent some harms from climate change if emissions reductions prove insufficient. Many
53 planetary-scale geoengineering approaches, however, present potentially considerable physical
54 risks and global governance challenges. While “geoengineering” has often referred only to
55 techniques that would have a substantial effect on the global-scale climate, in theory, certain
56 impacts could be geographically targeted using interventions that are limited in time and space.
57 The feasibility and efficacy of regional geoengineering approaches remain largely unexplored.

58 Here, as a proof-of-concept, we target an extensively researched regional teleconnection between
59 sea surface temperatures of the tropics and precipitation in the Sahel region of Africa ([Biasutti et
60 al., 2008](#)). The Sahel is home to approximately 100 million people, a number of vulnerable and
61 endangered species and a waypoint for many migratory birds. A multi-decadal drought in the
62 1970s and 80s resulted in famine, displacement and declines in regional biodiversity ([Mortimore,
63 2010; Walther, 2016](#)). While the consequences of climate change on mean Sahelian precipitation
64 and frequency and severity of intermittent drought are uncertain ([Giannini & Kaplan, 2019; Hill
65 et al., 2018](#)), the ability to protect the region from risk of future drought under global warming
66 could have a large humanitarian and ecological impact.

67 A robust observational and modeling literature supports the existence of teleconnections between
68 tropical SSTs and Sahelian precipitation ([Giannini et al., 2003; Lu & Delworth, 2005](#)). Multiple
69 factors have been examined to explain the drivers of the 20th century drought, including a shift in
70 the interhemispheric temperature gradients that determine the location of the intertropical
71 convergence zone (ITCZ) and teleconnection with the tropical oceans ([Michela Biasutti, 2019](#)).
72 Regardless of the causal mechanisms, studies have consistently identified an anomaly between
73 Northern-Southern hemispheric ocean temperatures as a feature of Sahel drought-period
74 climatology ([Giannini et al., 2013](#)).

75 Our modeled intervention mimics artificial upwelling activities, which were first proposed as a
76 means for carbon sequestration. Previous work demonstrates that, when implemented globally,
77 this would disrupt the thermocline and, on centennial timescales, lead to higher global mean
78 temperatures than if artificial upwelling had not been implemented in the first place
79 ([Kwiatkowski et al., 2015](#)). However, targeted deployment at regional and seasonal scales could
80 be used to change climate locally.

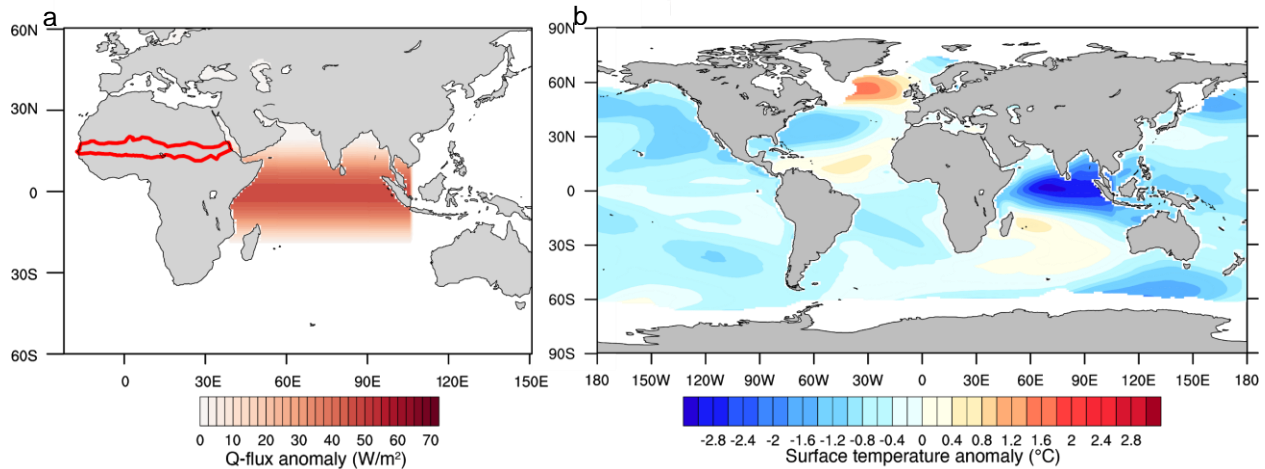
81 As a theoretical exploration of what a targeted regional climate intervention with artificial
82 upwelling could accomplish, we simulate surface cooling of the Indian Ocean and show that
83 such targeted cooling results in a sharp increase in Sahelian precipitation which increases
84 approximately linearly with the magnitude of regional forcing. To test the efficacy of the
85 targeted cooling in a more quasi-realistic intervention, we then apply the cooling response
86 derived in the idealized experiments to reverse the late 20th century Sahelian drought. While we
87 restore annual mean precipitation during the 1970s-80s in the historical intervention simulations,
88 we find that the seasonal and geographic distribution of precipitation is different than in the pre-
89 drought historical period. In addition, the intervention results in substantial precipitation side
90 effects elsewhere in the region. In particular, the full restoration of Sahelian precipitation during
91 the late 20th century drought is accompanied by a substantial reduction in precipitation in Sub-
92 Saharan East Africa.

93 **2 Idealized simulations to increase Sahelian precipitation**

94 We use the Community Earth System Model (CESM) version 1.2.2 with Community
95 Atmosphere Model version 5 (CAM5) ([Hurrell et al., 2013](#)) to conduct four idealized numerical
96 experiments (summarized in Table S1). For our idealized intervention simulations, we used the
97 “slab ocean” configuration of the model, wherein grid-cell level surface ocean heat fluxes are
98 prescribed. That is, while there is not a dynamic ocean there is still two-way energy exchange
99 between the atmosphere and ocean, with the lateral and vertical fluxes in and out of each slab
100 ocean grid box specified at the monthly time scale. As a result of the dynamic response of the
101 atmosphere, the geographic pattern of the surface temperature response to this “Q-flux”
102 perturbation does not directly correspond to the pattern of forcing.

103 In our reference simulations, global mean Q-flux is zero, with the forcing field mimicking the
104 observed ocean transport of energy from the tropics to higher latitudes. To place the outcomes in
105 our idealized Indian ocean cooling scenarios in the context of both pre-industrial and present day
106 climate, we conducted equilibrium reference simulations with both preindustrial concentrations
107 of atmospheric CO₂ (*ref_preind*) and doubled CO₂ (*ref_warm_world*). In our ocean cooling
108 simulations, we prescribe a net downward Q-flux to mimic the surface cooling that would occur
109 with ocean upwelling by artificially increasing transport of cold water from beneath the
110 thermocline and associated mixing and displacement of warm surface water. Figure 1a illustrates
111 the forcing perturbation made in our most extreme Indian Ocean cooling simulation
112 (*io_cooled_strongly*) with a positive zonally varied Q-flux perturbation over the region pictured
113 and reference flux (zero perturbation) elsewhere. This perturbation produces a global, annual
114 mean forcing of 1.6 W/m², but the peak local forcing across the center of the Indian Ocean is
115 much higher, approximately 47 W/m². While this is a large perturbation, the surface heat fluxes
116 are still of a comparable magnitude to natural background fluxes in the tropics, as illustrated in
117 Figure S1. The Q-flux perturbation induces strong surface cooling over the Indian Ocean, as
118 expected, as well as surface temperature changes elsewhere due to the dynamic response of the
119 atmosphere (Fig 1b). While the natural background Q-fluxes vary by month, identical
120 magnitudes of Q-flux perturbation were applied in all months throughout the simulations.

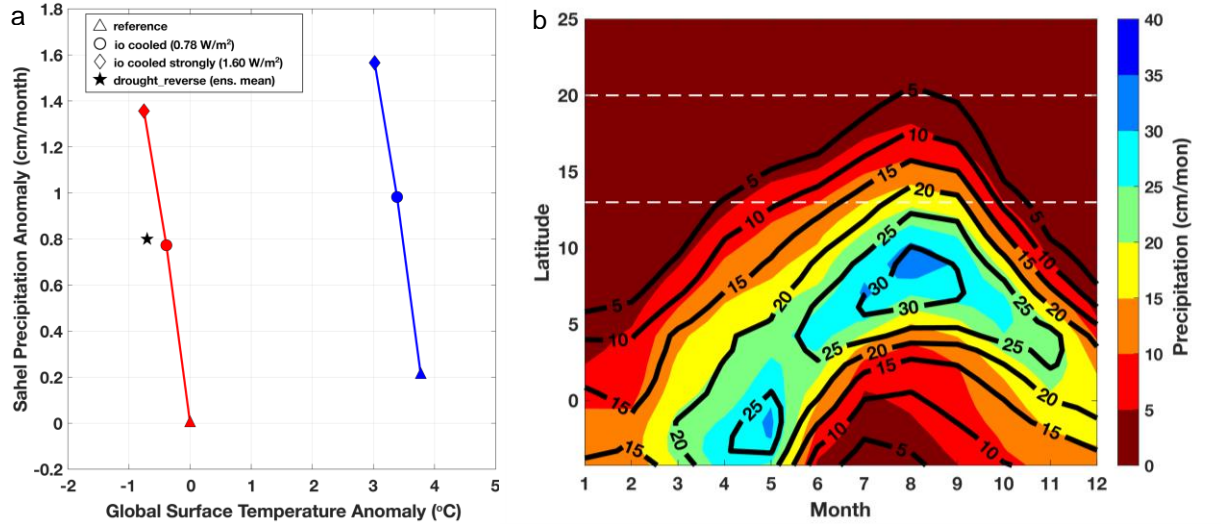
121



122 **Figure 1.** Simulation forcing perturbations to (a) surface heat flux (W/m^2) anomalies for *io_cooled_strongly* slab
 123 ocean experiments (anomaly is zero elsewhere) with the Sahel region outlined in red, and (b) surface temperature
 124 ($^{\circ}\text{C}$) anomalies induced by the *io_cooled_strongly* experiment, and applied as the perturbation to inputs for the
 125 *drought_reverse* prescribed SST experiments (see Section 3).
 126

127 The artificial upwelling intervention was designed to maximize increase in precipitation over the
 128 Sahel per decrease in global mean temperature. We conducted a perturbed simulation with half
 129 the Q-flux forcing (*io_cooled*) as well to examine the linearity of the forcing response. We find
 130 an approximately linear relationship between global mean surface temperature decrease, and
 131 Sahelian precipitation increase (Fig.2a). This relationship holds both in a pre-industrial
 132 (ref_preind) and in a greenhouse gas warmed world (re_warm_world). The outlined region in
 133 Figure 1a shows the region we define as the Sahel for the purposes of our efficacy analysis.
 134 Comparing first the two reference scenarios, we find that a world warmed by elevated
 135 atmospheric carbon dioxide has slightly higher, but substantially similar annual mean
 136 precipitation in the Sahel. When we increase the magnitude of heat transport into the deep Indian
 137 Ocean, and thereby cool SSTs (as illustrated in Fig 1), Sahelian precipitation increases with
 138 global temperature with an efficacy of $-1.8 \text{ cm/month}/^{\circ}\text{C}$ indicating a high sensitivity of Sahelian
 139 precipitation to global cooling concentrated in this particular region. This precipitation response
 140 to global temperature is markedly different from that associated with globally diffuse,
 141 greenhouse gas driven surface warming where cooling is associated with moderate drying
 142 (Sahelian precipitation efficacy of $0.06 \text{ cm/month}/^{\circ}\text{C}$).

143



144

145

146

147

148

Figure 2. Results of idealized simulations: a) relationship Sahel precipitation and global surface temperature anomalies in all simulations; b) monthly precipitation (cm/month) over Africa (20°W-30°E) by latitude and month, with *ref_warm_world* results in solid color and *io_strongly_cooled* in contour. (The latitudes associated with the Sahel region, (13-20°N,) marked in white)

149

150 There are two major climatological phenomena that drive the features of the annual hydrological
151 cycle in the Sahel: the annual migration of the Intertropical Convergence Zone (ITCZ) and the
152 annual African monsoon. The historical drought is thought to be driven primarily by a change in
153 interhemispheric forcing (Biasutti, 2019). Our drought restoration intervention is also achieved
154 primarily by widening the rainband over Africa, rather than through manipulation of the ITCZ
155 position in space and time (Fig 2b).

156 **3 Historical drought and drought reversal simulations**

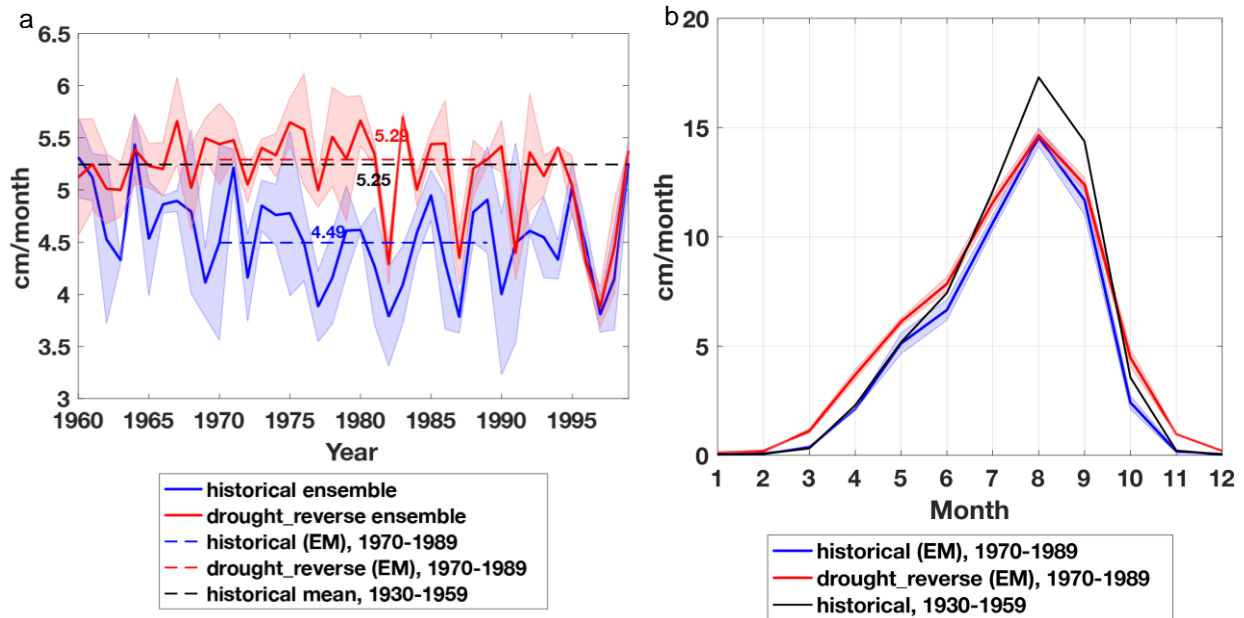
157 To illustrate the implications of our idealized intervention, the surface temperature anomalies
158 derived in the slab ocean experiments were superimposed on prescribed SST simulations of the
159 20th century historical drought in the Sahel. In these 20th century historical drought reversal
160 simulations, we run the CESM1.2.2/CAM5 model with a data ocean, wherein SSTs –typically
161 based on observations – are prescribed for every gridcell. Observed SSTs are based on Hadley
162 Centre Global Sea Ice and Sea Surface Temperature ([Rayner et al., 2003](#)) We ran two three-
163 member ensembles of prescribed SST simulations using historical observed SSTs (*historical*)
164 and the surface temperature anomalies derived from the slab experiments above (shown in
165 Figure 1b) for the drought reversal simulations (*drought_reverse*).

166 While precise definitions of the drought period vary, the 1970s and 80s are generally considered
167 the peak time period of the late 20th century drought (Dai et al., 2004). Historical experiments
168 using CAM5 reproduce 20th century precipitation variability in the Sahel reasonably well
169 (Monerie et al., 2017). in our historical prescribed SST ensemble, annual mean precipitation in
170 the region averaging 5.3 cm/month during the mid-century pre-drought period and 4.5 cm/month
171 during the period between 1970-89, a decrease of approximately 15%. By applying the surface
172 cooling pattern associated with the *io_cooled_strongly* experiment on top of historical SSTs,
173 Sahelian precipitation is restored to 5.3cm/month between 1970-89 (Fig 3a).

174 While the annual mean precipitation over the 1970-89 period in the drought-reversal simulations
175 matches almost exactly with the mid-century non-drought period precipitation, the seasonal
176 distribution of precipitation is distinct from that in the pre-drought historical. In particular, the

177 additional precipitation in the drought-reversal simulation is concentrated in the boreal spring
 178 months relative to the pre-drought historical (Fig3b). The distribution of regional climatological
 179 responses to Indian Ocean cooling is similar in the idealized slab ocean and historical prescribed
 180 SST simulations, however unlike the idealized simulations the intervention is ineffective at
 181 increasing summer precipitation in the Eastern Sahel in the fixed SST simulations (see Figure
 182 S2). This results in a substantially lower efficacy in Sahelian precipitation increase per degree of
 183 global cooling ($-1.1 \text{ cm/mon/}^{\circ}\text{C}$, see Fig 2a) than in the idealized design simulations.

184



185

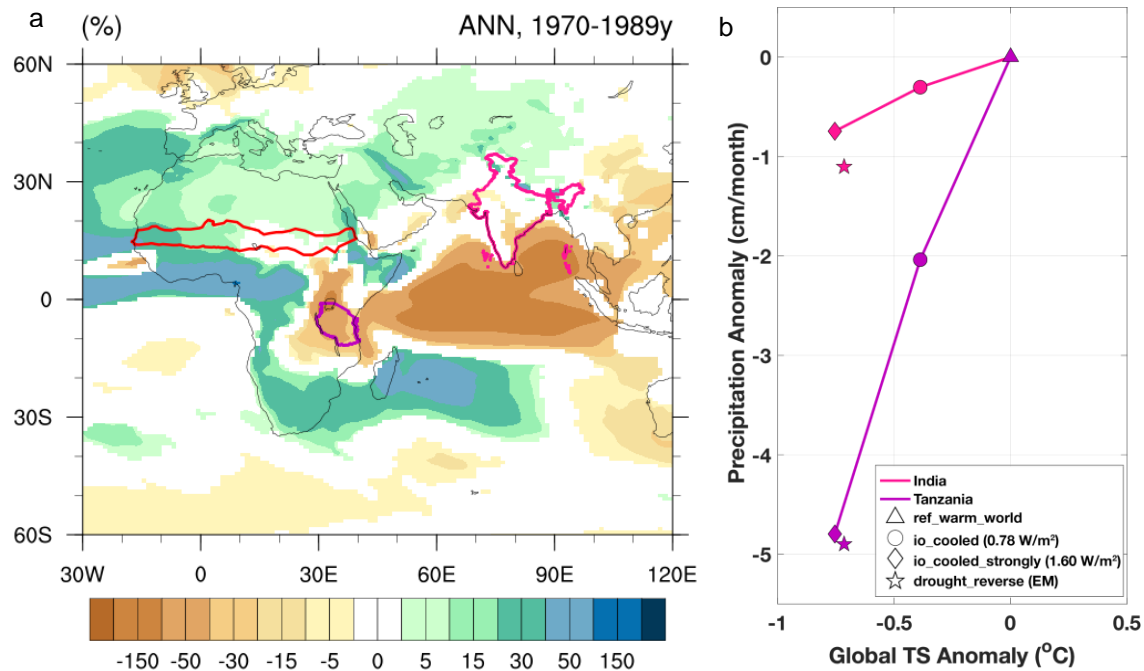
186 **Figure 3.** Sahel precipitation response in transient prescribed SST simulations: (a) time series of annual mean Sahel
 187 precipitation for the *historical* (blue) and *drought_reverse* (red) simulation ensembles, (b) annual cycles of monthly
 188 mean precipitation for the pre-drought *historical* (black), drought *historical* (blue) and *drought_reverse* (red).

189

190 A regional intervention like the one we design to mitigate drought in the Sahel is likely to have
 191 significant climatological effects beyond the target region. Indian Ocean cooling results in
 192 substantial effects on other proximate regional climates, including precipitation reductions in
 193 South and Southeast Asia, the southern Arabian Peninsula and, in particular, Sub-Saharan East
 194 Africa (Fig 4a). One might expect that substantial cooling over the Indian Ocean could have a
 195 large impact on precipitation over the Indian subcontinent through reduction of moisture
 196 availability and alteration of the monsoon dynamics. Comparing the reference simulations in

197 India, we find that a world warmed by elevated atmospheric carbon dioxide has higher
 198 temperature and precipitation. When we strongly cool the Indian Ocean, mean annual
 199 precipitation in India decreases with global surface temperature with an efficacy of
 200 1.5cm/month/°C (Fig 4b). This constitutes a small and statistically insignificant reduction
 201 compared to total mean precipitation over India. Some of the most substantial precipitation
 202 reductions occur in East Africa, particularly in and adjacent to Tanzania. In Tanzania, annual
 203 precipitation decreases with Indian Ocean cooling with an efficacy of 6.9cm/month/°C, a
 204 reduction that, in terms of percentage, is of similar magnitude to the increase in precipitation in
 205 the Sahel.

206



207

208 **Figure 4.** Distribution of precipitation anomalies associated with Indian Ocean cooling: a) Annual precipitation
 209 anomalies (%) maps from between SST prescribed experiments *drought_reverse* and *historical*. The bottom row are
 210 the differences (red-dryer, blue – wetter); b) global surface temperature vs precipitation anomalies in India (solid)
 211 and Tanzania (dashed).

212

213 **4 Feasibility scoping analysis**

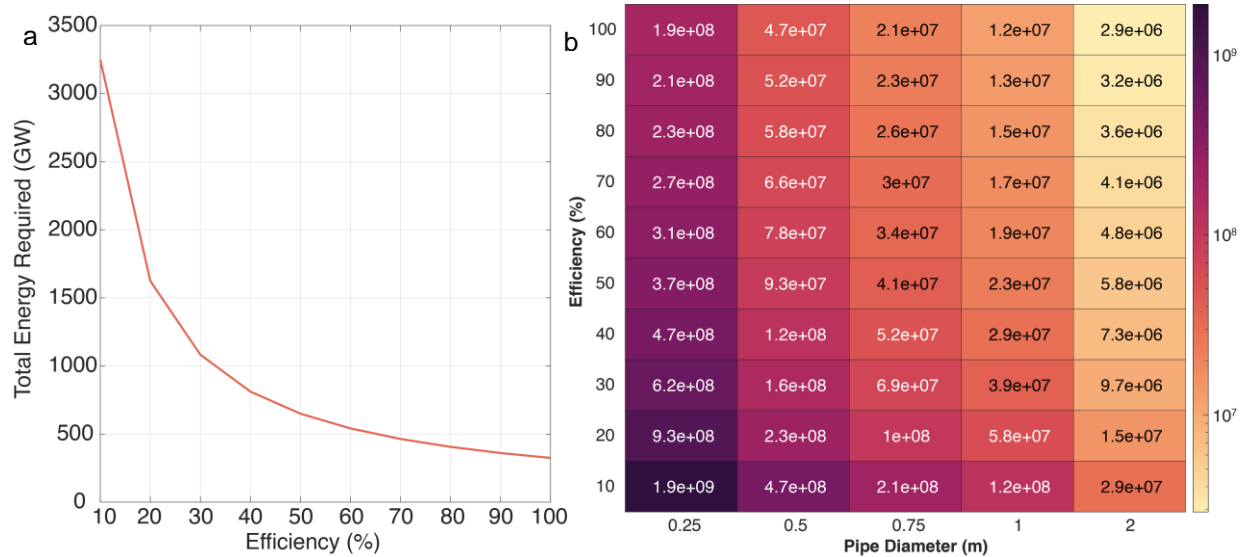
214 Our modeled regional climate intervention mimics artificial upwelling (AU), which was first
215 proposed as a means for carbon sequestration. By bringing nutrient-rich water from below the
216 thermocline to the surface, phytoplankton blooms could be stimulated and carbon captured
217 ([Lovelock & Rapley, 2007](#)). Earth system modeling work has suggested artificial upwelling
218 would not be an effective carbon sequestration method, however, due to the potential for CO₂
219 outgassing to the atmosphere from either high concentrations of dissolved inorganic carbon
220 pumped to the surface or the termination of pipe operation ([Oschlies et al., 2010](#); [Kwiatkowski et
221 al., 2015](#)). These experiments do demonstrate, however, that artificial upwelling has significant
222 thermodynamic impacts by cooling sea surface temperatures. Technologies designed to
223 implement artificial upwelling have been field tested and demonstrate the same thermal effects
224 ([White et al., 2010](#)). This suggests that artificial upwelling may be more plausibly deployed for
225 its cooling effects rather than biogeochemical ones.

226

227 While there is little doubt AU is theoretically possible, to implement it at the scale simulated
228 would require substantial investment and alteration of the physical environment. To provide a
229 preliminary analysis of the feasibility of a regional intervention like the one presented here, we
230 estimate energy and number of pipes required to cool the Indian Ocean by the same amount as in
231 the *drought_reverse* simulations. To do this, we utilized a linear first order differential equation
232 characterizing the change in heat at the surface as deep ocean water is upwelled to the mixed
233 layer while influenced by surface energy fluxes from the simulations (see Supporting Text). The
234 upwelling rates within a region were optimized by constraining the resulting heat loss at steady
235 state to the grid-cell level temperature anomalies from the *drought_reverse* simulations (Fig S3).
236 The regional upwelling rates are then constrained by typical upwelling rates of pipes and,
237 following a method similar to that of ([Fan et al., 2013](#)), the amount of energy and number of
238 pipes can then be determined. We estimate that cooling this region with 150m pipes with a 30%
239 efficiency would require approximately 1,000 GW (equivalent to about 9,000 TWh, or about
240 35% of global electricity consumption). Using 150m pipes that are 1 meter in diameter and with

241 30% efficiency, this would require approximately 40 million pipes (equivalent to 5.8 million km
 242 of pipe, nearly double the total length of all pipelines in the world).

243



244

245 **Figure 5.** Efficiency-dependent estimation of (a) annual-mean power required (GW) to realize a strong cooling of
 246 the Indian Ocean and (b) number of pipes required dependent on pipe diameter.

247

248 5 Limitations, discussion and conclusions

249 The results above represent a proof of concept. The regional intervention was designed though
 250 exploratory analysis and, while alternative regional boundaries for ocean cooling were
 251 investigated, we did not fully optimize our intervention to increase rain in the Sahel. The
 252 intervention was also not temporally tuned; thus, it's possible one could retain the positive
 253 outcomes in the Sahel and reduce impacts elsewhere by introducing seasonality, such as reduced
 254 cooling in the period March-May when the most drastic reductions in East African precipitation
 255 occur. In the historical drought reversal experiments, we assume that the surface temperature
 256 anomalies induced in the slab ocean experiments could be approximately reproduced spatially
 257 under more realistic conditions. Notably, these experiments do not include the dynamic response
 258 of the ocean which will be an important avenue of research in follow-up studies. Increased model
 259 resolution might also change regional hydrological outcomes substantially.

260 To our knowledge, this is the first study that has explored the possibility of targeting a climate
261 teleconnection with a climate intervention approach. We exploited one extensively studied
262 regional teleconnection between SSTs and precipitation over land, but the same approach could
263 be applicable to other dynamical systems or drought prone regions. Our approach requires some
264 understanding of the basic climate dynamics driving the regional hydroclimate in order for
265 regional scale interventions to be effective. Without such system understanding, the discovery of
266 sensitivities like the one between Indian Ocean temperature and Sahelian precipitation could
267 require infeasible amounts of trial-and-error. A lack of consideration of the dynamics could also
268 produce side effects that are greater than expected, though as the analysis of precipitation over
269 India reveals, whether side effects are perceived as positive or negative will depend on the
270 baseline of comparison.

271 There is a large and robust literature on climate teleconnections that could guide future studies
272 on the feasibility of targeted regional geoengineering (Liu & Alexander, 2007; Stan et al., 2017;
273 Yuan et al, 2018). The difference between a geoengineered teleconnection and those observed
274 and modeled in the existing literature is that natural modes of variability exhibit patterns of
275 spatial correlation that can theoretically be broken with a technology like artificial upwelling or
276 cloud brightening. More studies on the outcomes of interventions like the one explored in this
277 paper will be required in order to draw any conclusions about the feasibility and implications of
278 regional artificial upwelling interventions. The technical and political considerations that would
279 enter into any future decisions about deploying such approaches would undoubtedly be
280 extremely complex. However, there isn't a physical or geopolitical basis for assuming that global
281 rather than regional processes will determine future geoengineering activities. This suggests that
282 regional climate interventions aimed at mitigating particular risks associated with climate change
283 are underexplored in the geoengineering literature to date.

284

285 **Acknowledgments**

286 The CESM project is supported primarily by the National Science Foundation. We thank all the
287 scientists, software engineers, and administrators who contributed to the development of CESM.
288 An award of computer time was provided by the HPC@UC program at the San Diego

289 Supercomputer Center (SDSC). KR and DI were supported by funding from the Vetlesen
290 Foundation. TM is supported by an NSF Graduate Research Fellowship.

291

292 **Data Availability**

293 The CESM1.2.2 source code and input data are available through subversion code repositories
294 accessible through the model's public webpage: <https://www.cesm.ucar.edu/models/cesm1.2/> .

295 For the purposes of the review the data to produce the figures can be found here:

296 https://drive.google.com/drive/folders/1KP_KONFRijN80HdRzBIK681fCqX8PcFX?usp=sharing

297 [g](#). A DOI will be generated after acceptance.

298 **References**

299 Biasutti, M., Held, I. M., Sobel, A. H., & Giannini, A. (2008). SST Forcings and Sahel Rainfall Variability in
300 Simulations of the Twentieth and Twenty-First Centuries. *Journal of Climate*, 21(14), 3471–3486.

301 <https://doi.org/10.1175/2007JCLI1896.1>

302 Biasutti, Michela. (2019). Rainfall trends in the African Sahel: Characteristics, processes, and causes. *WIREs*
303 *Climate Change*, 10(4), e591. <https://doi.org/10.1002/wcc.591>

304 Boettcher, M., Chai, F., Cullen, J., Goeschl, T., Lampitt, R., Lenton, A., et al. (2019). *High Level Review of a Wide*
305 *Range of Proposed Marine Geoengineering Techniques* (Report). GESAMP. Retrieved from
306 [http://www.gesamp.org/publications/high-level-review-of-a-wide-range-of-proposed-marine-](http://www.gesamp.org/publications/high-level-review-of-a-wide-range-of-proposed-marine-geoengineering-techniques)
307 [geoengineering-techniques](http://www.gesamp.org/publications/high-level-review-of-a-wide-range-of-proposed-marine-geoengineering-techniques)

308 Dai, A., Lamb, P. J., Trenberth, K. E., Hulme, M., Jones, P. D., & Xie, P. (2004). The recent Sahel drought is real.
309 *International Journal of Climatology: A Journal of the Royal Meteorological Society*, 24(11), 1323-1331.

310 Fan, W., Chen, J., Pan, Y., Huang, H., Arthur Chen, C.-T., & Chen, Y. (2013). Experimental study on the
311 performance of an air-lift pump for artificial upwelling. *Ocean Engineering*, 59, 47–57.

312 <https://doi.org/10.1016/j.oceaneng.2012.11.014>

313 Giannini, A., Saravanan, R., & Chang, P. (2003). Oceanic Forcing of Sahel Rainfall on Interannual to Interdecadal
314 Time Scales. *Science*, 302(5647), 1027–1030. <https://doi.org/10.1126/science.1089357>

315 Giannini, A., Salack, S., Lodoun, T., Ali, A., Gaye, A. T., & Ndiaye, O. (2013). A unifying view of climate change
316 in the Sahel linking intra-seasonal, interannual and longer time scales. *Environmental Research Letters*,

- 317 8(2), 024010. <https://doi.org/10.1088/1748-9326/8/2/024010>
- 318 Giannini, Alessandra, & Kaplan, A. (2019). The role of aerosols and greenhouse gases in Sahel drought and
319 recovery. *Climatic Change*, 152(3), 449–466. <https://doi.org/10.1007/s10584-018-2341-9>
- 320 Griffiths, J. (2020, December 3). China to expand weather modification program to cover 5.5 million square
321 kilometers - CNN. Retrieved February 22, 2021, from [https://www.cnn.com/2020/12/03/asia/china-
322 weather-modification-cloud-seeding-intl-hnk/index.html](https://www.cnn.com/2020/12/03/asia/china-weather-modification-cloud-seeding-intl-hnk/index.html)
- 323 Hill, S. A., Ming, Y., & Zhao, M. (2018). Robust Responses of the Sahelian Hydrological Cycle to Global Warming.
324 *Journal of Climate*, 31(24), 9793–9814. <https://doi.org/10.1175/JCLI-D-18-0238.1>
- 325 Hurrell, J. W., Holland, M. M., Gent, P. R., Ghan, S., Kay, J. E., Kushner, P. J., et al. (2013). The Community Earth
326 System Model: A Framework for Collaborative Research. *Bulletin of the American Meteorological Society*,
327 94(9), 1339–1360. <https://doi.org/10.1175/BAMS-D-12-00121.1>
- 328 Johannessen, O. M., Subbaraju, G., & Blindheim, J. (1987). Seasonal variations of the
329 oceanographic conditions off the southwest coast of India during 1971-1975.
- 330 Kwiatkowski, L., Ricke, K. L., & Caldeira, K. (2015). Atmospheric consequences of disruption of the ocean
331 thermocline. *Environmental Research Letters*, 10(3), 034016. [https://doi.org/10.1088/1748-
332 9326/10/3/034016](https://doi.org/10.1088/1748-9326/10/3/034016)
- 333 Letelier, R. M., Strutton, P. G., & Karl, D. M. (2008). Physical and ecological uncertainties in the
334 widespread implementation of controlled upwelling in the North Pacific Subtropical Gyre. *Marine Ecology
335 Progress Series*, 371, 305-308.
- 336 Liu, Z., & Alexander, M. (2007). Atmospheric bridge, oceanic tunnel, and global climatic teleconnections. *Reviews
337 of Geophysics*, 45(2).
- 338 Lovelock, J. E., & Rapley, C. G. (2007). Ocean pipes could help the Earth to cure itself. *Nature*, 449, 403.
339 <https://doi.org/10.1038/449403a>
- 340 Lu, J., & Delworth, T. L. (2005). Oceanic forcing of the late 20th century Sahel drought. *Geophysical Research
341 Letters*, 32(22). <https://doi.org/10.1029/2005GL023316>
- 342 Monerie, P. A., Sanchez-Gomez, E., Pohl, B., Robson, J., & Dong, B. (2017). Impact of internal variability on
343 projections of Sahel precipitation change. *Environmental Research Letters*, 12(11), 114003.
- 344 Mortimore, M. (2010). Adapting to drought in the Sahel: Lessons for climate change. *WIREs Climate Change*, 1(1),

- 345 134–143. <https://doi.org/10.1002/wcc.25>
- 346 Oschlies, A., Pahlow, M., Yool, A., & Matear, R. J. (2010). Climate engineering by artificial ocean upwelling:
347 Channelling the sorcerer's apprentice. *Geophysical Research Letters*, *37*(4).
348 <https://doi.org/10.1029/2009GL041961>
- 349 Prasad, T. G., & Bahulayan, N. (1996). Mixed layer depth and thermocline climatology of the
350 Arabian Sea and western equatorial Indian Ocean.
- 351 Rayner, N. A., Parker, D. E., Horton, E. B., Folland, C. K., Alexander, L. V., Rowell, D. P., et al. (2003). Global
352 analyses of sea surface temperature, sea ice, and night marine air temperature since the late nineteenth
353 century. *Journal of Geophysical Research: Atmospheres*, *108*(D14). <https://doi.org/10.1029/2002JD002670>
- 354 Readfearn, G. (2020, April 16). Scientists trial cloud brightening equipment to shade and cool Great Barrier Reef.
355 Retrieved February 22, 2021, from [http://www.theguardian.com/environment/2020/apr/17/scientists-trial-](http://www.theguardian.com/environment/2020/apr/17/scientists-trial-cloud-brightening-equipment-to-shade-and-cool-great-barrier-reef)
356 [cloud-brightening-equipment-to-shade-and-cool-great-barrier-reef](http://www.theguardian.com/environment/2020/apr/17/scientists-trial-cloud-brightening-equipment-to-shade-and-cool-great-barrier-reef)
- 357 Stan, C., Straus, D. M., Frederiksen, J. S., Lin, H., Maloney, E. D., & Schumacher, C. (2017). Review of tropical-
358 extratropical teleconnections on intraseasonal time scales. *Reviews of Geophysics*, *55*(4), 902-937.
- 359 Walther, B. A. (2016). A review of recent ecological changes in the Sahel, with particular reference to land-use
360 change, plants, birds and mammals. *African Journal of Ecology*, *54*(3), 268–280.
361 <https://doi.org/10.1111/aje.12350>
- 362 White, A., Björkman, K., Grabowski, E., Letelier, R., Poulos, S., Watkins, B., & Karl, D. (2010). An Open Ocean
363 Trial of Controlled Upwelling Using Wave Pump Technology. *Journal of Atmospheric and Oceanic*
364 *Technology*, *27*(2), 385–396. <https://doi.org/10.1175/2009JTECHO679.1>
- 365 You, Y., & Tomczak, M. (1993). Thermocline circulation and ventilation in the Indian Ocean
366 derived from water mass analysis. *Deep Sea Research Part I: Oceanographic Research Papers*, *40*(1), 13-
367 56
- 368 Yuan, X., Kaplan, M. R., & Cane, M. A. (2018). The interconnected global climate system—A review of tropical-
369 polar teleconnections. *Journal of Climate*, *31*(15), 5765-5792.

370

371 **Supporting References**

- 372 Cole, S. T., Wortham, C., Kunze, E., & Owens, W. B. (2015). Eddy stirring and horizontal diffusivity from Argo

- 373 float observations: Geographic and depth variability. *Geophysical Research Letters*, 42(10), 3989-3997.
- 374 Fan, W., Chen, J., Pan, Y., Huang, H., Arthur Chen, C.-T., & Chen, Y. (2013). Experimental study on the
375 performance of an air-lift pump for artificial upwelling. *Ocean Engineering*, 59, 47–57.
376 <https://doi.org/10.1016/j.oceaneng.2012.11.014>
- 377 Liang, N. K., & Peng, H. K. (2005). A study of air-lift artificial upwelling. *Ocean engineering*,
378 32(5-6), 731-745.
- 379 Pan, Y., Fan, W., Huang, T. H., Wang, S. L., & Chen, C. T. A. (2015). Evaluation of the sinks and
380 sources of atmospheric CO₂ by artificial upwelling. *Science of the Total Environment*, 511, 692-702.
- 381 Pan, Y., Fan, W., Zhang, D., Chen, J., Huang, H., Liu, S., ... & Chen, Y. (2016). Research progress in
382 artificial upwelling and its potential environmental effects. *Science China Earth Sciences*, 59(2), 236-248.
- 383